Indian J. Phys. **75A** (1), 37-41 (2001)

IJP A
— an international journal

Effect of crystal orientation in GaAs on microwave negative and series positive resistances of flat profile DDR

S P Pati*, S Satapathy and S K Dash
Department of Physics, Sambalpur University,
Jyoti Vihar, Burla-768 019, Sambalpur, Orissa
E-mail sp_pati@hotmail.com

Abstract The ionization rate being one of the most influencing factors for the IMPATT diode operation, the effect of ionization rate of GaAs DDR (Double Drift Diode) along the different crystal orientation has been analyzed The analysis predicts a better microwave performance from the <111> oriented GaAs IMPATT in comparison to the <100> and <110> oriented device

Keywords Microwave performance, GaAs IMPATT diodes, ionization rate

PACS Nos. 84 40 -x, 07.57.-c

1. Introduction

IMPATT diodes are basically negative resistance oscillators capable of producing microwaves to sub-millimeter waves. The wide range of frequency covered by this device has pushed its importance with regard to various communication systems. The negative resistance at microwave frequency is produced through incorporation of phase difference between RF voltage and RF current in the range of $\pi/2$ to $3\pi/2$. Transit time taken by the charge carriers to traverse the drift region and the avalanche phase delay produced in the avalanche build up process of charge carriers resulting the requisite phase difference in case of IMPATT diodes. Amongst the two physical processes, which generate condition for RF oscillation, the avalanche build up process depends on the carrier ionization rate in a semiconductor. The ionization rate field characteristics are typical of the semiconductor and usually determined by the band structure of the corresponding semiconductors. The band structure of GaAs, which is a promising material for IMPATT diode fabrication, has been reported to depend on crystal orientation *i.e.* E ~ k diagram has been observed to be different for <111>, <100>, <110> oriented GaAs. Pearsall *et al* [1] have accounted for this effect and have experimentally determined the electron and hole ionization rates in GaAs along different crystal orientation. It is interesting to observe that the carrier ionization rates are widely different along the three orientation. Since the avalanche build up process and the avalanche delay produced by such process depend on ionization rate, the authors plan to study the microwave properties of GaAs IMPATT diodes along three different crystal orientations. Double drift diodes for operation in the V-band have been designed and analyzed through use of a computer simulation method, for determination of microwave properties along the different crystal orientation. It is interesting to observe that <111> orientation may become a preferred orientation for the fabrication of IMPATT diodes.

* Corresponding Author
All symbols are defined in the Appendix.

2. Method

The static and small signal analyses have been carried out by using computer simulation methods. At first, the DC analysis has been done through use of a double iterative computer simulation program [2, 5] which simultaneously solves Poisson's equation

$$\delta E / \delta x = q / \varepsilon \{p - n + N_D - N_A\} \quad (1)$$

and combined carrier continuity equation

$$\delta / \delta t (p+n) = q^{-1} \delta / \delta x (J_n - J_p) + 2(a_p v_p p + a_n v_n n), \quad (2)$$

where the carrier densities for electron and hole are given as, $J_n = q.v_n.n$ and $J_p = q.v_p.p$ and the total current density $J = J_n + J_p$. For static condition, eq. (2) becomes,

$$q^{-1} \delta / \delta x (J_n - J_p) + 2(a_p v_p p + a_n v_n n) = 0. \quad (3)$$

Defining $P(x) = \{J_p(x) - J_n(x)\} / J$, the eq. in (3) will take form:

$$\delta P(x) / \delta x = (a_n + a_p) - (a_n - a_p) P(x) \quad (4)$$

and

$$q\{\delta(p-n) / \delta x\} = -q(a_n - a_p)(p-n) + J(a_n / v_p + a_p / v_n) + (\delta E / \delta x) K, \quad (5)$$

where K is a correction factor whose value depends upon the nature of the velocity – field characteristics in a semiconductor. For silicon,

$$v_{n,p} = v_{sn,sp}\left[1 - \exp(\mu_{n,p} E / v_{sn,sp})\right]$$

and the correction factor K can be found out to be

$$K = (J_p \mu_p) / v_p \{1 / v_{sp} - 1 / v_p\} - (J_n \mu_n) / v_n \{1 / v_{sn} - 1 / v_n\}. \quad (6)$$

The field and carrier current profiles of the IMPATT diode can be obtained from the solution of eq. (1), (4) and (5) by applying proper boundary conditions. The boundary condition is that at the left edge of the depletion layer, the hole current comprises of only the reverse saturation current J_{sp} which enters the depletion layer at this point.

Thus at $x = x_L$,

$$P(x) = \{(J_p - J_n) / J\} = \{J_{sp} - (J - J_{sp})\} / J = (2 J_{sp} / J) - 1. \quad (7)$$

Taking the hole multiplication factor to be $M_p = J / J_{sp}$, eq. (7) becomes

$$P(x_L) = (2 / M_p) - 1.$$

Similarly at the right hand side edge where the electron current comprises of only the reverse saturation current J_{sn} and entering at that point,

$P(x_R) = 1 - (2 / M_n)$, where electron multiplication factor $M_n = J / J_{sn}$.

In addition to above, the field boundary conditions are to be satisfied which is given as

$$E(x_L) = E(x_R) = 0.$$

The different zone widths like avalanche zone width, drift zone width, the respective voltage drop V_A, V_D and V_B *etc* are obtained from integration of electric field profile across different zones. The edges of depletion layer are also determined accurately from the DC analysis and are taken as starting and end point for computation of small signal analysis. The device efficiency has been calculated using the relation $\eta = V_D / \pi V_B$. Taking the DC data as input, the small signal analysis has been carried out. The analysis involves the simultaneous solution of the two integrated second order differential equations in diode negative resistance (R) and reactance (X) [3, 6] which are given as

$$D^2 R + (a_n - a_p) DR - 2r\omega \bar{v} DX + \{(\omega \bar{v}^{-1})^2 - H(x)\} R - 2a\omega v^{-1} X = 2\bar{a}(v\varepsilon)^{-1}, \quad (8)$$

$$D^2 X + (a_n - a_p) DX - 2r\omega \bar{v}^{-1} DR + \{(\omega \bar{v}^{-1})^2 - H(x)\} X + 2a\omega \bar{v}^{-1} R = -\omega(\bar{v}^2 \varepsilon)^{-1}, \quad (9)$$

where the quantities, $\bar{v}$, $\bar{a}$, r, H and D are defined as

$$\bar{v} = (v_{sn} \cdot v_{sp})^{1/2}, \quad \bar{a} = (a_n v_{sn} + a_p v_{sp}) / 2\bar{v}, \quad r = (v_{sn} - v_{sp}) / 2\bar{v},$$

$$H = (2J / \bar{v}\varepsilon)\delta\bar{a} / \delta E + (\delta / \delta E)(a_p - a_n)(\delta E_m / \delta X)$$

and $D = \delta / \delta x$.

The equations are solved by taking the proper boundary conditions [6]

$$\varepsilon\{(\delta R / \delta x) - (\omega X / v_{sp})\} = 1 / v_{sp};$$

$$(\delta X / \delta x) + (\omega R / v_{sp}) = 0 \quad (10)$$

at the boundary of the p-region and

$$\varepsilon\{(\delta R / \delta x) - (\omega X / v_{sn})\} = -1 / v_{sn};$$

$$(\delta X / \delta x) - (\omega R / v_{sn}) = 0 \quad (11)$$

at the boundary of n-region.

The computer simulation method that the authors have followed is double iterative over the initial choice of values of R and X at the left edge of the depletion layer. At first some arbitrary values of R and X are choosen at $x = x_L$ and the values of DR and DX are determined using the eq. (10). Knowing this values of R, X, DR, DX at $x = x_L$, one can determine the values of these parameters at $x = x_L + dx$ by using modified Runge-Kutta method. This process is repeated to determine the values of R, X, DR, DX at subsequent steps till the other end $x = x_R$ is reached. The boundary conditions given in the eq. (11) are then compared with the values computed at $x = x_R$. If the conditions are not satisfied then the initial values at $x = x_L$ are suitably changed to repeat the numerical solution of equation (8 and 9). The values of R and X can be changed in four different ways as, $R \rightarrow R \pm \delta R$ and $X \rightarrow X \pm \delta X$ for consecutive iterations. A fast logic has been framed to ensure early convergence.

The final solution gives spatial distribution of R and X and the integrated values of resistance and reactance are obtained as,

$$Z_R = \int R(x)\, dx \quad \text{and} \quad Z_X = \int X(x)\, dx.$$

The device negative conductance (G), device susceptance (B) and quality factor (Q) are calculated using the relation,

$$G = Z_R\left(Z_R^2 + Z_X^2\right)^{-1},\quad B = -Z_X\left(Z_R^2 + Z_X^2\right)^{-1}$$

and $Q = |B/G|$.

In addition to the microwave negative resistance, the diode also generates some positive series resistance. This positive RF series resistance arises from n^+/p^+ substrate, metal semiconductor contact, undepleted epilayer and device packaging *etc*. The value of the series resistance may some time become comparable to the microwave negative resistance generated at high frequency operation of the IMPATT diode and therefore may become responsible for generation of low RF oscillating power from device mainly due to the cancellation of the usual high frequency negative resistance. Therefore it is desirable to keep the positive resistance value to be low. The diode positive resistance is calculated using the relation [4]

$$g = -G - B^2 R_s.$$

The analysis has been carried out using the method described above. The method is made realistic by considering realistic impurity profile across the junction and incorporating realistic variation of carrier ionization rates and drift velocities in silicon with electric field and temperature. The space step width is taken to be very small such that there are more than 1000/nm steps for the entire depletion zone layer of the diode. The method is made free from numerical instability and less time consuming through incorporation of a fast converging logic.

2.1 Material parameters

2.1.1. Ionization rate

The ionization rate data along different crystal orientation have been measured and reported by Pearsall *et al* [1], which can be fitted into an exponential field variation of the form

$$a_{n,p} = A_{n,p} \exp\left[-(b_{n,p}/E)^m E\right].$$

The variation of ionization rate with electric field has been shown in Figure 1.

2.1.2. Other material parameters

The other material parameters are :

$V_{sn} = 8.0 \times 10^4\ \text{ms}^{-1}$, $V_{sp} = 1.0 \times 10^4\ \text{ms}^{-1}$, $E_c = 0.65 \times 10^6\ \text{Vm}^{-1}$, $\mu_n = 0.85\ \text{m}^2\text{V}^{-1}\text{s}^{-1}$, $\mu_p = 0.04\ \text{m}^2\text{V}^{-1}\text{s}^{-1}$, $\epsilon = 1.16 \times 10^{-10}\ \text{Fm}^{-1}$, $E_g = 1.42\ \text{eV}$, $m^*/m_0 = 0.037$.

3. Results and discussion

The GaAs DDR IMPATT diodes have been designed and the diode structural parameters have been optimized by using a computer iterative method and considering localization of avalanche zone width. (x_A/W), maximum efficiency (η) and optimum punch through factor. The optimized design parameters

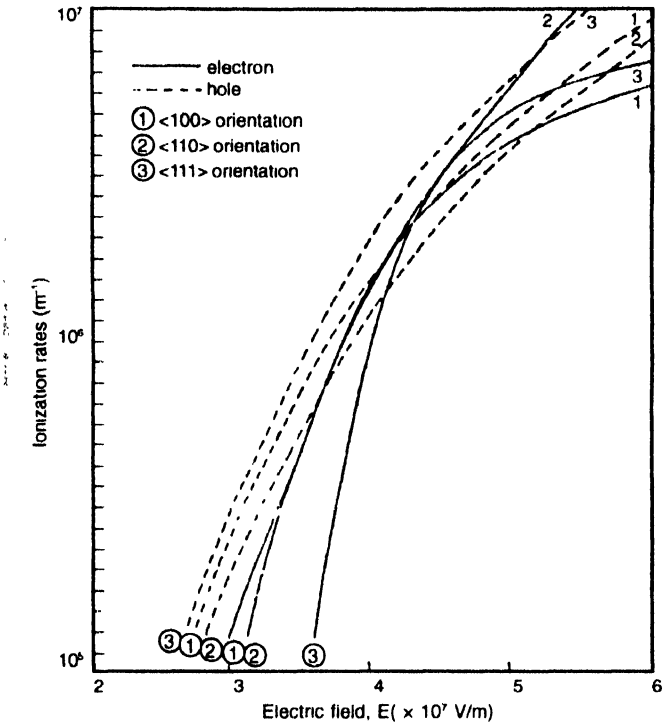

Figure 1. Electric field dependence of carrier ionization rates for different crystal orientations of GaAs.

are $W_n = 730$ nm, $W_p = 880$ nm, $N_D = 0.5 \times 10^{23}/\text{m}^3$, $N_A = 0.4 \times 10^{23}/\text{m}^3$, $J_0 = 1.0 \times 10^8\ \text{A/m}^2$. The DC and small-signal results have been listed in Tables 2 and 3 respectively. Table 1 shows that the maximum electric field E_0 of the DDR diodes are slightly different for the three crystal orientation. The junction field is the maximum for <100> orientation.

Table 1. DC results of GaAs DDR IMPATT.

Orientation	E_0 (10^7 A/m^2)	V_B (V)	(η) (%)	x_A/W
<111>	4 47	41 7	17 4	0 292
<100>	4 81	42 7	15 2	0 344
<110>	4 80	43 2	15.3	0 348

The device efficiency is observed to be the highest for the <111> orientation. The efficiency of the <100> and <110> orientation are nearly equal to each other. The avalanche zone width (x_A/W) is the lowest for the <111> orientation followed by the <100> and <110> orientations. Thus the DC analysis predicts better microwave characteristics for the <111> oriented GaAs DDR diode.

The small signal properties are shown in Table 2 and Figures 2 and 3. The Figure 2 shows the G-B plots and Figure 3 shows

Table 2. Small signal characteristics for GaAs DDR diode for different crystal orientation

Orientation	F (GHz)	G (10^6 S/m^2)	R_s (10^{-7} Ωm^2)	θ_s (π rad)
<111>	50	3 51	0 567	0 482
	60	13 0	0 329	0 473
	80	8 41	0.261	0 420
	100	2 21	0 009	0 400
<100>	50	8 02	0 851	0 481
	55	8 77	0 369	0 443
	80	4 43	0 344	0 390
	100	1 17	0 321	0 388
<110>	50	6 47	1 76	0 443
	60	8 21	0 299	0 378
	80	5 81	0 070	0 330
	100	1 62	0.053	0 313

the R(x) profiles for the different crystal orientation. Figure 2 shows that the peak value of the device negative conductance is maximum for the <111> oriented GaAs DDR. The device negative resistance is also found to be the highest for <111> oriented GaAs DDR. The device positive series resistance is lower for the <111> structure as it can be observed from Table 2. The highest value of the negative resistance observed in case of <111> oriented GaAs IMPATT diode can be explained on the basis of the ionization rate profile shown in Figure 1. It can be observed from the ionization rate profile (Figure 1) that for all the crystal orientations the ionization rate is nearly equal for

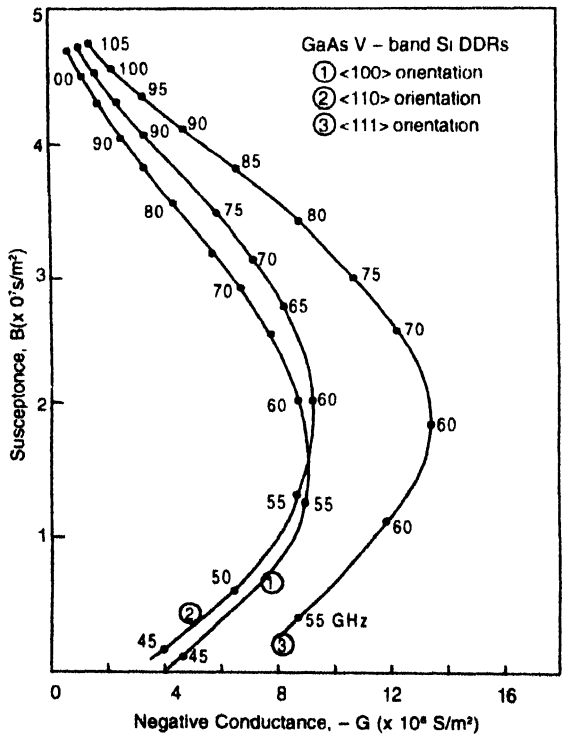

Figure 2. Negative conductance vrs susceptance plots for different crystal orientations of V – band GaAs DDRs

electrons around an electric field value of 4.5×10^7 V/m, whereas it is widely different for holes. The ionization rates of holes are found to be the highest for <111> oriented GaAs for the entire electric field range in the depletion layer of the diode, which causes localization of avalanche zone width, thereby increasing the drift zone width, which increases the avalanche phase delay More is the avalanche phase delay, greater will be the negative resistance. The value of the positive resistance increases for higher frequency bands (> 100 GHz) whereas it is negligible for lower frequency bands (<30 GHz). But the negative resistance increases with higher band of operation. Therefore, it is preferable to operate the diode within this range of frequency to realize more output power.

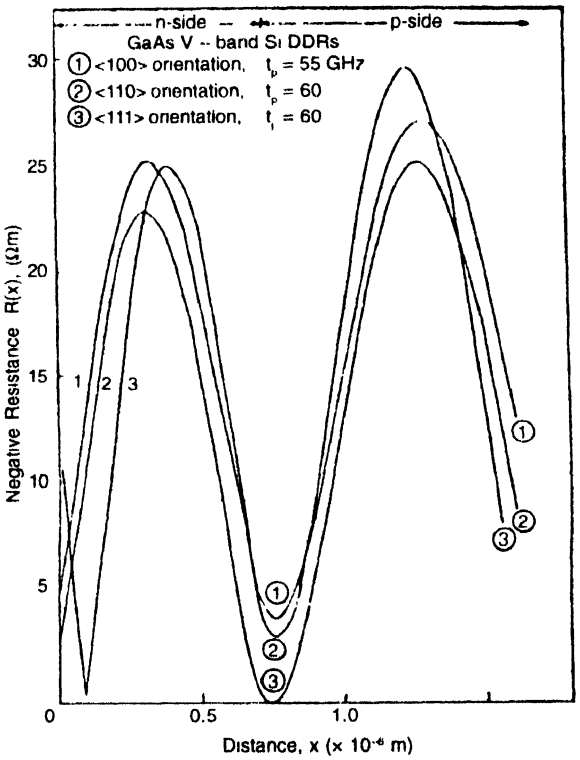

Figure 3. Negative resistance profiles for different crystal orientations of GaAs V–band DDR

4. Conclusion

The highest value of negative resistance and lowest value of positive resistance make the <111> oriented GaAs IMPATT diode the more promising one for microwave power generation.

Acknowledgment

The author Ms Sasmita Satpathy wishes to thank the Council of Scientific & Industrial Research, India for awarding Senior Research Fellowship (Extended) in her favour.

References

[1] T P Pearsall, F Capasso, R E Nohory, A Pollack and J R Chelikowsky *Solid State Electron.* **21** 297 (1978)

[2] S P Pati, S Satpathy, A K Panda and G N Dash *Indian J. Phys* **69A** 183 (1995)

[3] A K Panda, G N Dash, S Satpathy and S P Pati *Phys Stat Sol (a)* **54** 657 (1996)

[4] M G Adlestein, L H Holway and S L G Chu *IEEE Trans On Electron. Devices* **ED-30** 179 (1983)

[5] D N Datta, S P Pati, B B Pal and S K Roy *IEEE Trans on Electron. Devices* **Ed-29** 1813 (1982)

[6] S P Pati, J P Banerjee and S K Roy *J. Phys.* **D22** 959 (1989)

Appendix

List of Symbols :

B	Diode susceptance	(S/m^2)
E,E(x)	Electric field at any space point	(V/m)
E_m	Electric field associated with mobile space charge only	(V/m)
E_0	Value of field maximum	(V/m)
F	Frequency	(GHz)
G	Diode conductance	(S/m^2)
G_p	Peak value of negative conductance	(S/m^2)
J	Total current density (A/m^2)	
N_D	Donor doping concentration	(m^{-3})
N_A	Acceptor doping concentration	(m^{-3})
n	Electron concentration	(m^{-3})
p	Hole concentration	(m^{-3})
q	Electronic charge	(C)
R,R(x)	Diode resistance at any space point	(Ωm)
V_A	Avalanche voltage drop	(V)
V_B	Breakdown voltage drop	(V)
V_D	Drift voltage drop	(V)
V	Carrier velocity	(ms^{-1})
v_n	Electron velocity at any field value E	(ms^{-1})
v_{sn}	Saturated drift velocity (electron)	(ms^{-1})
v_p	Hole velocity at any field value E	(ms^{-1})
v_{sp}	Saturated drift velocity (hole)	(ms^{-1})
W	Total depletion layer width	(nm)
x_A	Avalanche layer width	(nm)
Z	Diode impedance	(Ωm^2)
Z_R	Diode resistance	(Ωm^2)
Z_X	Diode reactance	(Ωm^2)
a_n	Electron ionisation rate	(m^{-1})
a_p	Hole ionisation rate	(m^{-1})
ε	Permittivity of semiconductor	(F/m)
μ_n	Electron mobility	(m^2/Vs)
μ_p	Hole mobility	(m^2/Vs)
ω	Angular frequency of rf current/voltage	(rad/s)
η	DC to rf conversion efficiency	